

Comparison the effects of chitosan and hyaluronic acid-based thermally sensitive hydrogels containing rosuvastatin on human osteoblast-like MG-63 cells

Vajihe Akbari¹, Mahboubeh Rezazadeh^{2,*}, and Zahra Ebrahimi²

¹Department of Pharmaceutical Biothenology, Isfahan Pharmaceutical Research Center, School of Pharmacy and Pharmaceutical Sciences, Isfahan University of Medical Sciences, Isfahan, I. R. Iran.

²Department of Pharmaceutics and Novel Drug Delivery System Research Center, School of Pharmacy and Pharmaceutical Sciences, Isfahan University of Medical Sciences, Isfahan, I.R. Iran.

Abstract

Background and purpose: Bone regeneration can be accelerated by localized delivery of statins. Here, we aimed to evaluate the effect of two thermosensitive hydrogels containing rosuvastatin (RSV) on proliferation and differentiation of human osteoblast-like MG-63 cells.

Experimental approach: Firstly, chitosan (CTS)/glycerophosphate (GP)/gelatin (G) thermosensitive hydrogel was prepared and characterized based on rheological properties, *in vitro* erosion, and release pattern of RSV and then the optimized mixture was loaded with nanoparticles containing RSV(NRSV). Secondly, the effect of NRSV-embedded in CTS/GP/G on cell viability, alkaline phosphate activity, and cell calcification was evaluated using MG-63 cells and compared with RSV-embedded into hyaluronic acid (HA)/Pluronic[®] F127 (PF127) hydrogel.

Findings / Results: CTS/GP mixtures with 1 and 1.5 % gelatin existing in solution with low viscosity at 4 °C were solidified at 32-34 °C while the mixture containing 2% gelatin was jellified at room temperature. The gelation times of CTS/GP/G with 1 and 1.5% gelatin were 72 and 44 s, respectively. The hydrogel containing 3% w/v NRSV was also converted to a semisolid upon increasing the temperature to 33-36 °C. Due to the higher gel strength of CTS/GP/G compared to HA/PF127 hydrogel, the release rate of RSV from the NRSV-embedded CTS/GP/G hydrogel was significantly slower than that of HA/PF127 system. As revealed by alkaline phosphatase and mineralization assays, NRSV-embedded in CTS/GP/G hydrogel had the most promotive effect on differentiation of osteoblasts among other mixtures.

Conclusion and implication: NRSV-embedded in CTS/GP/G hydrogel could be efficiently used in the future for bone defects such as osteoporosis and bone fractures.

Keywords: Rosuvastatin; Thermosensitive hydrogel; Tissue engineering.

INTRODUCTION

Treatment of bone defects such as bone fractures and bone loss in some disease such as osteoporosis has still remained a major clinical problem (1). Although growth factors such as bone morphogenetic protein-2 (BMP-2) has been widely evaluated for bone repair (2,3), the low physiological stability of these biological factors has so far hindered their practical application. Additionally, the high molecular weight of proteins and their complex structures could induce unwanted reaction of immune system in patients (4). There are some recent reports which show that

statins, synthetic lipid lowering agents, have potential to stimulate bone regeneration, *via* alteration of bone metabolism pathways (5-7). Statins have been demonstrated to promote osteoblastic activity and inhibit osteoclastic activity through increasing the synthesis and secretion a wide ranges of factors and matrix proteins such as BMP-2. It is also reported that statins decrease the secretion of pro-inflammatory cytokines such as interleukin-6 and interleukin-8 (5,7).

*Corresponding author: M. Rezazadeh
Tel: +98-3137927123, Fax: +98-3136680011
Email: rezazade@pharm.mui.ac.ir

Access this article online



Website: <http://rps.mui.ac.ir>

DOI: 10.4103/1735-5362.278719

Several types of statin drugs are available in market to treat hypercholesterolemia. Following oral ingestion, statins are extensively metabolized in the liver and their bioavailability is estimated less than 20% (8). Thus, effective bone defect healing would not be achieved by oral delivery of statins. Nevertheless, positive effects of statins in bone regeneration have been illustrated following oral ingestion (9,10). Based on literature review, localized sustained administration of statins in bone sites would enhance their efficacy in bone reconstruction (11-14). However, most of earlier published reports have focused on local delivery of lipophilic statins such as lovastatin and simvastatin (12,13,15). The results of recent investigations have demonstrated that rosuvastatin (RSV) and pravastatin as hydrophilic statins are more efficient than lipophilic ones in terms of proliferation and mineralization (14,16). For instances, RSV-loaded sponges implanted into fractured rat femora promoted new bone formation with high mineral density (17,18). In another similar research, a biodegradable polymeric implant was used as a carrier for localized delivery of RSV to bone sites (19). In all aforementioned studies, because of high hydrophilicity and the low molecular weight of RSV, the drug content was completely released during 12 h. Ideally, a delivery system should provide a slow release of statins to achieve a beneficial effect on bone healing. In addition, all of previously developed carriers for delivery of RSV should be applied following invasive surgery in bone sites. Recently, we formulated RSV-loaded chitosan (CTS)/chondroitin sulfate (CS) nanoparticles (NRSV), which released RSV at a slow rate and the optimized nanoparticles were incorporated into hyaluronic acid (HA)/Pluronic® F127 (PF127) thermosensitive hydrogel to be locally applied in bone sites (20). Thermosensitive hydrogels are clinically desired, as these systems are liquid at room temperature and could be easily injected in bone sites, while upon exposure to the body temperature they solidify into a hydrogel drug depot. Considering the unique advantages of CTS as a scaffold in tissue regeneration, in the current work we prepared CTS-based

thermally sensitive hydrogel engrafted with NRSV and compared the effect of these two different delivery systems (CTS-based hydrogel versus HA-based hydrogel) on proliferation of osteoblast-like MG-63 cells. Here, the mixture of CTS, β -glycerophosphate (GP), and gelatin (G), was prepared and characterized as a thermosensitive hydrogel and loaded with NRSV. Given the cell proliferation activity of RSV, HA, and CTS, it seemed interesting to compare the effect of the HA-based and CTS-based delivery systems on proliferation of MG-63 cells, alkaline phosphatase activity (ALK), and cell calcification. Finally, the injectability of the most effective formulation was also characterized.

MATERIALS AND METHODS

RSV calcium, CTS (deacetylation degree: 85%, viscosity: 20-300 cP, molecular weight (M_w): 50-190 kDa), CS, HA, ($M_w = 100-150$ kDa), PF127 (polyoxyethylene-polyoxypropylene-polyoxyethylene tri-block copolymer, $M_w = 12.5$ kDa), G, and β -GP disodium salt were provided from Sigma Chemical Co. (St. Louis, MO, USA). Dulbecco's modified eagle's minimal essential medium (DMEM), fetal bovine serum (FBS) and penicillin-streptomycin (100 IU/mL and 100 μ g/mL, respectively) were obtained from Biosera (France). Human osteoblast-like MG-63 cells line was purchased from Pasteur institute (Tehran, I.R. Iran). 3-(4,5-Dimethylthiazol-2-yl)-2,5-diphenyltetrazolium bromide (MTT), Alizarin red, and Triton™ 100X were supplied by Sigma-Aldrich (St. Louis, MO, USA).

Preparation and characterization of thermosensitive NRSV-embedded CTS/GP/G solution

NRSVs were prepared and characterized as described in our previous work (20). Briefly, 5 mL of CTS solution with concentration 0.63 mg/mL in acetic acid at pH 4 slowly added to the 10 mL of CS solution at 1 mg/mL in which 0.5 mg RSV was already dissolved. The resulting suspension

was ultrasonicated using a probe sonicator (Baldelin, Berlin, Germany) and centrifuged in Faclon® tubes for 10 min at 3000 rpm (Hettich Zentrifugen Model Routine 420 g) to precipitate NRSV. The precipitate was then washed twice with deionized water and lyophilized to obtain white powder of NRSVs using freeze dryer (Model ALPHA 2-4 LD plus, Christ Company, Stuttgart, Germany). The size and zeta potential of the nanoparticles were determined by dynamic light scattering using a Zetasizer (3000HS, Malvern Instruments Ltd., Worcestershire, UK). The drug entrapment efficiency (EE), drug loading (DL), and release rate of RSV from nanoparticles were calculated according to our previous work (20). To prepare CTS/GP/G hydrogel solution, chitosan 2.5 % with 1, 1.5, or 2% (w/v) gelatin were dissolved in 0.1 M acetic acid at pH 3. Aqueous solution of GP was added to the CTS/G solution in a drop-wise manner at 4 °C and constant stirring. The final pH of the solution was adjusted to 7.4 (21). NRSV-embedded hydrogel was obtained by dispersing freeze-dried of NRSV into CTS/GP/G solution at concentration of 3 % w/v of the nanoparticles.

Rheological measurement of CTS/GP/G solution

Gelation temperature, gelation time, and the viscosities were measured using a digital rotary viscometer (RVDV-III U, Daiki Sciences Co. USA). Aqueous solutions of the hydrogels at 4 °C were transferred into the glass container of the viscometer attached to a controllable circulation water bath. Then, the temperature was gradually increased and the interval for measurement was 0.2 °C.

In vitro gel erosion behavior

Erosion of NRSV-embedded CTS/GP/G system was evaluated with respect to weight loss. Weight loss of initially weighed hydrogel (W_0) was monitored as a function of incubation time in BPS at 37 °C. At 3, 8, 24, 48, and 72 h, hydrogel were removed from phosphate buffered solution (PBS), freeze-dried, and then weighed (W_t) (22).

The weight loss ratio was defined as follows:

$$x = \frac{W_0 - W_t}{W_0} \times 100 \quad (1)$$

In vitro release studies of RSV from CTS and HA-based hydrogels

One mL of hydrogel solutions containing NRSV were placed in 25-mL flat-bottomed glass beakers and allowed to gel in an incubator at 37 °C for 5 min. Then, 10 mL PBS (0.1 M, pH 7.4) was poured on the surface of gels and the vessels were shaken in a water bath shaker at 40 rpm and 37 °C. At predetermined time points, 2 mL sample of the supernatant solution was withdrawn and replaced with 2 mL fresh buffer. RSV in the samples was measured using UV-visible spectrophotometer at wavelength 240 nm.

Cytotoxicity study

MG-63 cells were grown in DMEM containing 10% FBS and 1% penicillin-streptomycin at 37 °C and 5% CO₂. Cells were subcultured regularly using trypsin/EDTA. Cell suspension (200 µL at 5×10^5 cell/mL) was added to 200 µL of various formulations including, NRSV, NRSV-embedded CTS/GP/G hydrogel, the hydrogel without NRSV, and CTS/CS nanoparticles without RSV in 24-well plate. The plate was incubated for formation of physical gel at 37 °C for 30 min. After that, 1000 µL of fresh medium was added to each well and the plate was incubated for 1, 2, and 3 days. The plate also had one well with untreated cells as the negative control and one well with culture medium as the blank. For survival assay, 100 µL of MTT solution was poured into each well and the plate was kept in the incubator for 3 h at 37 °C. The medium/MTT mixtures were replaced by 800 µL of DMSO to dissolve the formazan crystals in cells. Finally, the absorbance was determined at 570 nm by a plate reader (Stat Fax-2100; Awareness Technology Inc., Palm City, FL, USA). Each experiment was performed three times to ensure reproducibility of results.

The percentage of cell survival for each well was determined by following equation (21).

$$\text{Cell survival (\%)} = \frac{\text{Mean absorbance of sample} - \text{mean absorbance of blank}}{\text{Mean absorbance of negative control} - \text{mean absorbance of blank}} \times 100 \quad (2)$$

Alkaline phosphatase activity

Alkaline phosphates activity as a functional feature for differentiation of MG-63 was determined for each sample using alkaline phosphatase kit (Pars Azmoon, I.R. Iran) according to manufacturer's instructions. Briefly, 200 μL of cell suspension (5×10^5 cell/mL) were added to 200 μL of the various hydrogels in 24-well plate. The plate was incubated for formation of physical gel at 37 $^{\circ}\text{C}$ for 30 min. Then, 1000 μL of fresh medium was poured into each well and the plate was incubated for 48 h. Then, culture medium was removed, the well was washed twice with PBS and cell lysis was performed by 0.1% Triton[®] 100X. The activity of enzyme in the supernatant of cell lysate was determined by a colorimetric quantitative assay using *p*-nitrophenyl phosphate as the substrate. The absorbance was measured at 405 nm by a plate reader (Stat Fax-2100; Awareness Technology Inc., Palm City, FL, USA). Each experiment was performed in triplicate (23).

Mineralization assay

Alizarin red staining was used to evaluate the degree of mineralization, another biochemical feature for differentiation of MG-63. The hydrogels (200 μL) was added to cell suspension; after gel formation, the sample incubated for 2 days. Next, culture medium was removed; the cells were washed with PBS two times; cell fixation was performed by incubation of cells with 4% formaldehyde at room temperature for 20 min. Two additional wash with PBS were performed and Alizarin solution (40 mM, pH 4) was added to each well and incubated for 60 min. Finally the wells were washed for four times with PBS and observed under an optical microscope and photographed using a digital camera (23).

Determination of injectability

The injectability of the optimized formulation was measured by means of a Texture Analyser (TA, Stable Micro System[®],

Vienna Court, UK) using fresh chicken meat to miming the injection into subcutaneous and muscles. The chicken meat was fixed in the sample holder of the apparatus, the hydrogel was filled into a 2-mL syringe with 21G needle (0.8 mm \times 40 mm), and fixed between the upper movable carriage and sample holder of the apparatus. The movable carriage was moved downward at a prefixed speed of 100 mm/min to inject the needle into the chicken meat. To determine the injection force of the formulation into a subcutaneous and muscles tissues, the needle was inserted 0.1 and 0.5 inch underneath the chicken skin, respectively (22).

Statistical analysis

Analysis Data were expressed as means of three separate experiments and were compared by independent sample t-test for two groups, and one-way ANOVA for multiple groups. A *P* value < 0.05 was considered statistically significant in all cases.

RESULTS

Rheological behavior of the CTS/G/GP hydrogel system

CTS/GP mixtures with 1 and 1.5% gelatin existed in solution with low viscosity at 4 $^{\circ}\text{C}$ which were converted to semisolid gels when the temperature was increased to 35 $^{\circ}\text{C}$. The *in vitro* morphology of the CTS/GP/G hydrogel system at room temperature and 37 $^{\circ}\text{C}$ is shown in Fig. 1A.

Gelation temperature and gelation time were also evaluated by measuring the viscosity versus temperature and time, respectively (Fig. 1B and C). The mixtures of CTS/GP with 1 or 1.5% gelatin were solidified at 32-34 $^{\circ}\text{C}$ while the mixture containing 2% gelatin was jellified at room temperature. The data relative to 1% gelatin is not shown as it exhibited the same rheological behavior as the solution containing 1.5% gelatin. Figure 1C represents viscosity versus time of CTS/GP/G with 1 and 1.5% gelatin at 30-35 $^{\circ}\text{C}$. The solution based on 1.5% gelatin solidified more quickly than the solution with 1% gelatin as evidenced by the higher rate in increasing the viscosity from the beginning of the measure. The gelation times of CTS/GP/G with 1 and 1.5% gelatin were 72 and 44 s, respectively. The gelation

behavior of CTS/GP/G after incorporation 3% RSV-loaded nanoparticles was similar to Fig.

1B with a slight increase in gelation time (data are not shown).

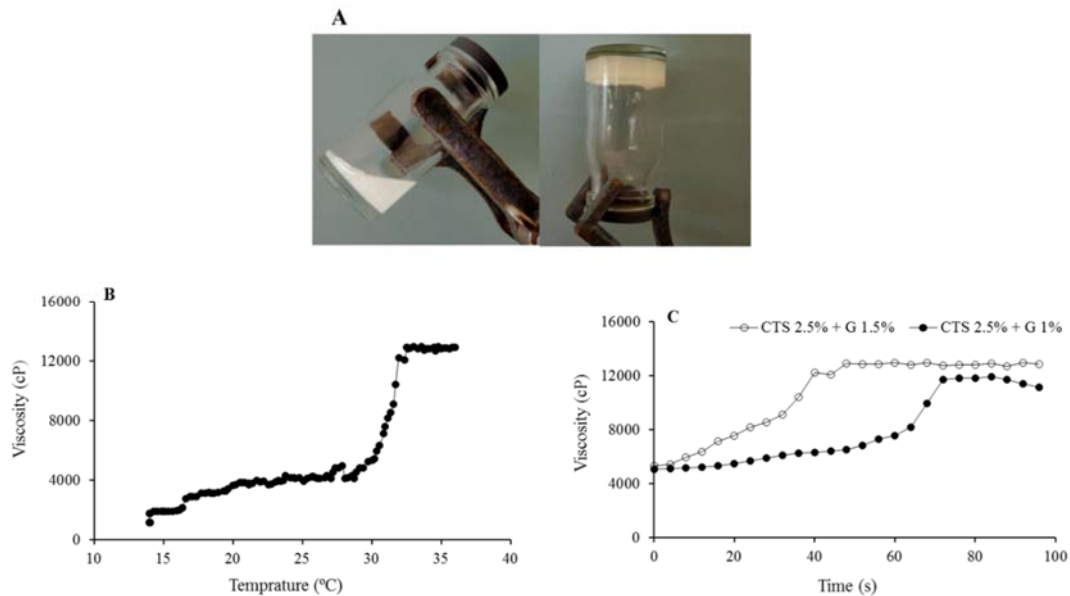


Fig. 1. (A) Visual observation of CTS/GP/G hydrogel at room temperature (left) and at 37 °C (right), (B) viscosity vs temperature of CTS/GP mixture with 1.5 % G, and (C) viscosity vs time of CTS/GP solutions with 1 and 1.5% G. CTS, chitosan; GP, glycerophosphate; G, gelatin.

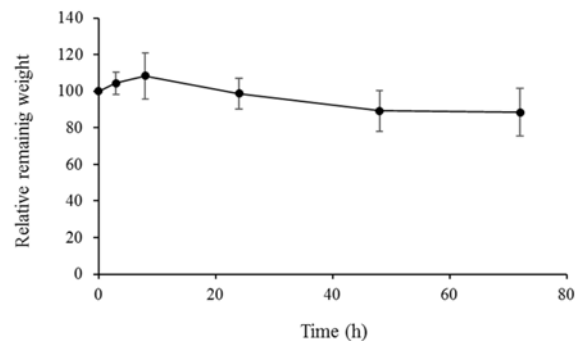


Fig. 2. The mass erosion behavior of chitosan/glycerophosphate/gelatin hydrogel system. Data represent the mean \pm SD, n = 3.

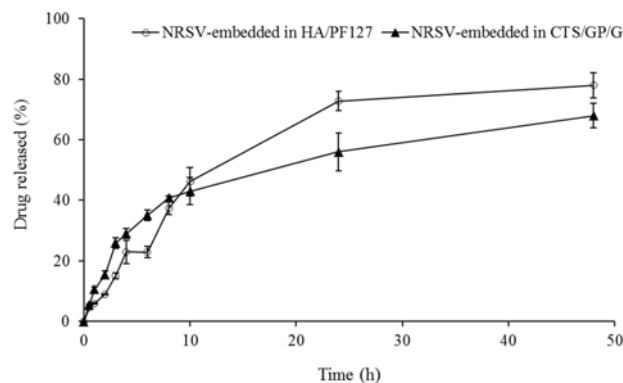


Fig. 3. *In vitro* release profiles of RSV from NRSV-embedded in HA/PF127 and NRSV-embedded in CTS/GP/G hydrogels. Data represent the mean \pm SD, n = 3. NRSV, Nanoparticles containing rosuvastatin; HA, hyaluronic acid; PF127, Pluronic® F127; CTS, chitosan; GP, glycerophosphate; G, gelatin.

In vitro gel erosion

Figure 2 shows the erosion behaviors of the hydrogel at 37 °C. CTS/GP/G maintained 85% of its original weight over 72 days, while the HA/PF127 hydrogel evaluated in our previous work (20) eroded to less than 70% of its initial weight during 3 days.

In vitro release studies of RSV from CTS and HA-based hydrogel

Figure 3 shows the cumulative release of RSV from NRSV-embedded in CTS/GP/G and HA/PF127 hydrogels. The cumulative drug release profile of RSV from the CTS/GP/G hydrogel was slower than that of HA/PF127 system. The mean release time values of NRSV-embedded in CTS/GP/G and HA/PF127 hydrogels were obtained 24.61 and 15.21 h, respectively.

Cytotoxicity assay

As shown in Fig. 4A, in comparison with blank CTS/CS nanoparticles, NRSV could increase survival and growth of MG-63, particularly after 72 h ($P \leq 0.05$). NRSV-embedded CTS/GP/G and blank CTS/GP/G could maintain the cell viability during incubation time.

Alkaline phosphatase activity

As revealed in Fig. 4B, alkaline phosphatase activity for cells seeded on NRSV-embedded CTS/GP/G was

significantly higher than NRSV-embedded HA/PF127 at 48 h and 72 h ($P \leq 0.05$). On the day three, MG-63 cells cultured in NRSV-embedded CTS/GP/G also showed more enzyme activity compared to CTS/GP/G ones ($P < 0.001$). MG-63 cells cultured in NRSV well exhibited more alkaline phosphatase activity compared with blank CTS/CS after 48 and 72 h ($P < 0.05$). It is clear from Fig. 4B, that alkaline phosphatase activity of the cells was enhanced by increasing the incubation time in all of the studied groups except HA/PF127 hydrogel.

Mineralization assay

Alizarin staining confirmed the results of alkaline phosphatase assay (Fig. 5). Cells incubated with NRSV-embedded CTS/GP/G or CTS/GP/G exhibited more calcium mineral content compared with other samples. Incubation of cells with NRSV or CTS/CS led to increase in calcium content compared with untreated cells. Furthermore, in comparison with the blank hydrogels, embedding NRSV into hydrogels led to stronger Alizarin staining.

Determination of injectability

The force required for injection of the CTS/GP/G hydrogel solution into subcutaneous and muscle tissue were 16.3 ± 2.5 and 17.8 ± 4.5 N, respectively indicating ease of formulation injection.

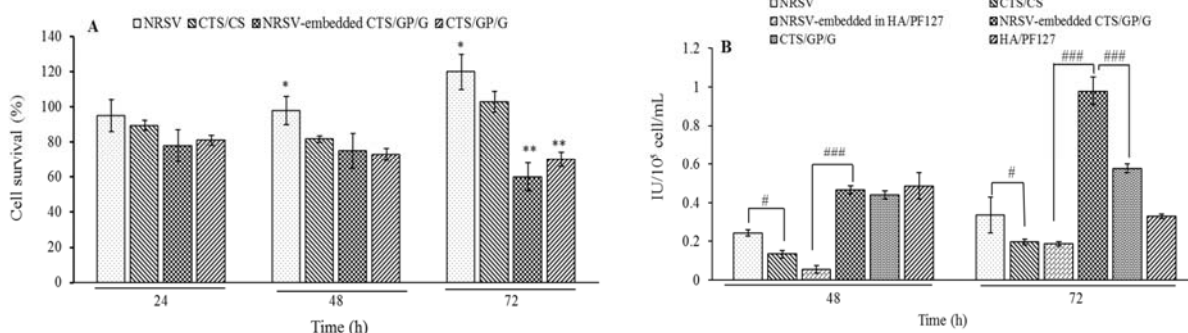


Fig. 4. (A) *In vitro* cytotoxicity of the different formulations against human osteoblast-like MG-63 cells and (B) ALK activity of MG-63 cells after 48 and 72 h of culture with NRSV, CTS/CS, NRSV-embedded in CTS/GP/G or CTS/GP/G. Data represent the mean \pm SD, n = 3. * $P \leq 0.05$ and ** $P \leq 0.01$ indicate significant differences compared with blank CTS/CS; # $P \leq 0.05$ and ### $P \leq 0.001$ show significant differences between defined groups. NRSV, Nanoparticles containing rosuvastatin; HA, hyaluronic acid; PF127, Pluronic® F127; CTS, chitosan; GP, glycerophosphate; G, gelatin; ALK, alkaline phosphatase.

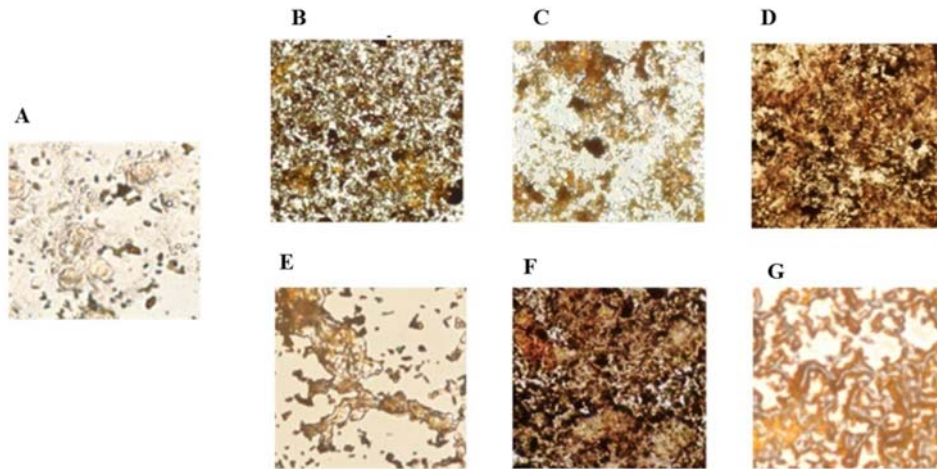


Fig. 5. Photographs of mineral deposition visualized by Alizarin Red staining. Cells were cultured for 48 h with (A) untreated cells, (B) CTS/CS, (C) NRSV, (D) NRSV-embedded CTS/GP/G, (E) NRSV-embedded HA/PF127, (F) CTS/GP/G, and (G) HA/PF127. NRSV, Nanoparticles containing rosuvastatin; HA, hyaluronic acid; PF127, Pluronic® F127; CTS, chitosan; GP, glycerophosphate; G, gelatin.

DISCUSSION

In the current study, we aimed to compare the efficacy of two different thermally sensitive hydrogels for sustained and localized delivery of RSV. The formulations were constructed through the incorporation of NRSV into HA/PF127 or CTS/GP/G hydrogel systems. In our previous study NRSV-embedded HA/F127 was successfully prepared and it converted to gel at 37 °C within a relative short time (20). Here, we developed another hydrogel system for local delivery of RSV and compared cytological features of these two delivery systems using human osteoblast cell line, MG-63. The results of rheological measurements indicated that CTS/GP/G containing 1 and 1.5% gelatin could be solidified at 32 °C. However, the system with 2% gelatin existed in a high viscous solution at 25 °C. The higher release rate of RSV from NRSV-embedded HA/PF127 compared to CTS/GP/G hydrogel especially at the later times could be attributed to higher gel strength of CTS/GP/G and its higher resistant to the mass erosion compared to HA/PF127 hydrogel. Based on literature review, RSV has a biphasic effect on the growth of osteoblast cells; it could improve cell survival at low concentrations ($\leq 0.01 \mu\text{M}$) while at high concentrations it could result in cell death

($\geq 10 \mu\text{M}$) (16). Here, NRSV led to higher cell viability compared with free RSV at RSV concentration of about $0.2 \mu\text{M}$. It could be due to the release pattern of RSV from the nanoparticles resulting in lower concentration of the drug and improvement of MG-63 survival. Previous studies reported that release kinetics of statins from carriers could also affect differentiation of osteoblasts (4). It is important to choose an appropriate delivery system, which provides slow and sustained release of statins to ensure increase in osteogenesis and preventing of inflammatory reaction (23). As revealed by alkaline phosphatase and mineralization assays, NRSV-embedded in CTS/GP/G hydrogel had the most promotive effect on differentiation of osteoblasts among other mixtures studied in the current work. It could be explained by the fact that this scaffold had slowest release rate of the drug among investigated matrices. Cell adhesion and attachment to the surface of hydrogel is also critical for proliferation and differentiation of anchorage-dependent cells like MG-63. Cell adhesion is highly dependent on physiochemical and biomechanical properties of scaffolds. It was observed that osteoblast seeded on CTS/GP/G hydrogels showed more cell viability compared with HA/PF127 ones evaluated in our previous study (20).

Viability for cells seeded on CTS/GP/G hydrogels was found to be 70-81% while cell viability of 59-71% was reported for HA/PF127 hydrogels. CTS is a biodegradable and poly-cationic biopolymer which could support cell adhesion, differentiation and proliferation (24). Mechanical strength and structural integrity of CTS-based hydrogels make them suitable for bone tissue engineering (24,25). Gelatin (denatured collagen), another component used in CTS/GP/G hydrogel, has similar biological properties to collagen while it is less expensive. Therefore, this biomaterial has been widely used as a collagen alternative for tissue engineering applications. Furthermore, gelatin has some specific binding domains (e.g. RDG) which facilitate cell attachment and adhesion (26). Moreover, addition of gelatin into the scaffold results in improvement of activity and differentiation of osteoblasts. On the other hand, HA especially its high molecular weight inhibits cell adhesion, proliferation, migration and angiogenesis. This natural polymer is widely applied in osteoarthritis and plastic surgery as an anti-adhesive agent (27). In the present study, lower cell viability observed for HA/PF127 hydrogel could be attributed to anti-adhesive property of HA. In agreement with our results, other groups reported that non-functionalized HA-based hydrogels could not support cell attachment and proliferation (28). Anti-adhesive properties of HA hydrogel could be explained based on its negative charge repelling cells. Another component of HA/PF127 hydrogel was pluronic F-127, a nonionic surfactant polyol. This agent could also be responsible for the decrease in viability of MG-63 seeded following incubation with HA/PF127 hydrogel. Similarly, Buttner *et al.* reported that pluronic F-127 polymer reduced cell viability of osteoblasts without change in their phenotype. However, treatment of this polymeric scaffold with platelet-rich plasma resulted in improvement of cell survival (29). Despite the unique advantages of HA for tissue engineering, our findings revealed that HA/PF127 thermally sensitive hydrogel

may not be a good scaffold for *in vitro* osteoblast proliferation. However, this hydrogel improved differentiation of osteoblasts, which may be due to biological properties of HA like mediating extracellular matrix remodeling. Based on our results, this novel tissue engineering scaffold, NRSV-embedded CTS/GP/G, can provide appropriate 3D microenvironment architectures for better osteoblast cell adhesion, differentiation and proliferation. This thermo-sensitive and injectable hydrogel scaffold can be considered as a promising candidate for bone tissue engineering which require further *in vivo* research to confirm the effectiveness, biocompatibility and maintenance of structural integrity of the hydrogel.

CONCLUSION

In this study, NRSV-embedded CTS/GP/G hydrogel with sustained release profile was prepared and evaluated for different physicochemical properties such as rheological behavior, *in vitro* erosion, and release rate of RSV, and then compared its effect on proliferation and mineralization of MG63 cells with HA/PF127 containing NRSV for bone tissue engineering application. Our results revealed that NRSV-embedded in CTS/GP/G hydrogel had the most promotive effect on differentiation and mineralization of osteoblasts among other studied mixtures. It can be concluded that NRSV-embedded in CTS/GP/G hydrogel may be used clinically in the future for bone defects such as osteoporosis and bone fractures, because they have better bioavailability and bioactivity than free RSV. However, more intensive studies are still needed to confirm the *in vivo* effectiveness, biocompatibility, and maintenance of structural integrity of the hydrogel.

ACKNOWLEDGMENTS

The content of this paper is extracted from the Pharm. D thesis submitted by Zahra Ebrahimi which was financially supported (No. 395851) by the Vice

Chancellery of Research of Isfahan University of Medical Sciences, Isfahan, I.R. Iran.

CONFLICT OF INTEREST STATEMENT

The authors declare no conflict of interest for this study.

AUTHORS' CONTRIBUTION

All authors contributed equally in this work.

REFERENCES

- Gittens SA, Uludag H. Growth factor delivery for bone tissue engineering. *J Drug Target.* 2001;9(6):407-429.
- Bessa PC, Casal M, Reis RL. Bone morphogenetic proteins in tissue engineering: the road from laboratory to clinic, part II (BMP delivery). *J Tissue Eng Regen Med.* 2008;2(2-3):81-96.
- Shields LB, Raque GH, Glassman SD, Campbell M, Vitaz T, Harpring J, *et al.* Adverse effects associated with high-dose recombinant human bone morphogenetic protein-2 use in anterior cervical spine fusion. *Spine (Phila Pa 1976).* 2006;31(5):542-547.
- Park YS, David AE, Park KM, Lin CY, Than KD, Lee K, *et al.* Controlled release of simvastatin from *in situ* forming hydrogel triggers bone formation in MC3T3-E1 cells. *AAPS J.* 2013;15(2):367-376.
- Yue J, Zhang X, Dong B, Yang M. Statins and bone health in post-menopausal women: a systematic review of randomized controlled trials. *Menopause.* 2010;17(5):1071-1079.
- Toh S, Hernández-Díaz S. Statins and fracture risk. A systematic review. *Pharmacoepidemiol Drug Saf.* 2007;16(6):627-640.
- Maeda T, Matsunuma A, Kawane T, Horiuchi N. Simvastatin promotes osteoblast differentiation and mineralization in MC3T3-E1 cells. *Biochem Biophys Res Commun.* 2001;280(3):874-877.
- Ayukawa Y, Yasukawa E, Moriyama Y, Ogino Y, Wada H, Atsuta I, *et al.* Local application of statin promotes bone repair through the suppression of osteoclasts and the enhancement of osteoblasts at bone-healing sites in rats. *Oral Surg Oral Med Oral Pathol Oral Radiol Endod.* 2009;107(3):336-342.
- Nyan M, Sato D, Oda M, Machida T, Kobayashi H, Nakamura T, *et al.* Bone formation with the combination of simvastatin and calcium sulfate in critical-sized rat calvarial defect. *J Pharmacol Sci.* 2007;104(4):384-386.
- Moriyama Y, Ayukawa Y, Ogino Y, Atsuta I, Koyano K. Topical application of statin affects bone healing around implants. *Clin Oral Implants Res.* 2008;19(6):600-605.
- Lee Y, Chung HJ, Yeo S, Ahn CH, Lee H, Messersmith PB, *et al.* Thermosensitive injectable and tissue adhesive sol-gel transition hyaluronic acid/pluronic composite hydrogel prepared from bio-inspired catechol-thiol reaction. *Soft Matter.* 2010;6(5):977-983.
- Yoshii T, Hafeman AE, Esparza JM, Okawa A, Gutierrez G, Guelcher SA. Local injection of lovastatin in biodegradable polyurethane scaffolds enhances bone regeneration in a critical-sized segmental defect in rat femora. *J Tissue Eng Regen Med.* 2014;8(8):589-595.
- Dolkart O, Pritsch T, Sharfman Z, Somjen D, Salai M, Maman E, *et al.* The effects of lipophilic and hydrophilic statins on bone tissue mineralization in saos2 human bone cell line-*in vitro* comparative study. *Pharm Anal Acta.* 2015;6(5):1-4.
- Ertugrul DT, Yavuz B, Cil H, Ata N, Akin KO, Kucukazman M. STATIN-D study: comparison of the influences of rosuvastatin and fluvastatin treatment on the levels of 25-hydroxyvitamin D. *Cardiovasc Ther.* 2011;29(2):146-152.
- Lee Y, Schmid MJ, Marx DB, Beatty MW, Cullen DM, Collins ME, *et al.* The effect of local simvastatin delivery strategies on mandibular bone formation *in vivo*. *Biomaterials.* 2008;29(12):1940-1949.
- Monjo M, Rubert M, Ellingsen JE, Lyngstadaas SP. Rosuvastatin promotes osteoblast differentiation and regulates SLC01A1 transporter gene expression in MC3T3-E1 cells. *Cell Physiol Biochem.* 2010;26(4-5):647-656.
- Ibrahim HK, Fahmy RH. Localized rosuvastatin via implantable bioerodible sponge and its potential role in augmenting bone healing and regeneration. *Drug Deliv.* 2016;23(9):3181-3192.
- Dong C, Yu B, Hu ZB, Zhou ZL, Yang H, Jin AM. Rosuvastatin implant for local bone specific drug delivery in osteoporotic bone fracture. *J Biomater Tissue Eng.* 2015;5(7):565-569.
- Porter JR, Ruckh TT, Popat KC. Bone tissue engineering: a review in bone biomimetics and drug delivery strategies. *Biotechnol Prog.* 2009;25(6):1539-1560.
- Rezazadeh M, Parande M, Akbari V, Ebrahimi Z, Taheri A. Incorporation of rosuvastatin-loaded chitosan/chondroitin sulfate nanoparticles into a thermosensitive hydrogel for bone tissue engineering: preparation, characterization, and cellular behavior. *Pharm Dev Technol.* 2019;24(3):357-367.
- Cheng YH, Yang SH, Su WY, Chen YC, Yang KC, Cheng WT, *et al.* Thermosensitive chitosan-gelatin-glycerol phosphate hydrogels as a cell carrier for nucleus pulposus regeneration: an *in vitro* study. *Tissue Eng Part A.* 2010;16(2):695-703.

22. Rezazadeh M, Akbari V, Amuaghae E, Emami J. Preparation and characterization of an injectable thermosensitive hydrogel for simultaneous delivery of paclitaxel and doxorubicin. *Res Pharm Sci*. 2018;13(3):181-191.
23. Martin PD, Warwick MJ, Dane AL, Brindley C, Short T. Absolute oral bioavailability of rosuvastatin in healthy white adult male volunteers. *Clin Ther*. 2003;25(10):2553-2563.
24. Croisier F, Jérôme C. Chitosan-based biomaterials for tissue engineering. *Eur Polym J*. 2013;49:780-792.
25. Yu P, Bao RY, Shi XJ, Yang W, Yang MB. Self-assembled high-strength hydroxyapatite/graphene oxide/chitosan composite hydrogel for bone tissue engineering. *Carbohydr Polym*. 2017;155:507-515.
26. Perez RA, Del Valle S, Altankov G, Ginebra MP. Porous hydroxyapatite and gelatin/hydroxyapatite microspheres obtained by calcium phosphate cement emulsion. *J Biomed Mater Res B Appl Biomater*. 2011;97(1):156-166.
27. Kogan G, Šoltés L, Stern R, Gemeiner P. Hyaluronic acid: a natural biopolymer with a broad range of biomedical and industrial applications. *Biotechnol Lett*. 2007;29:17-25.
28. Park YD, Tirelli N, Hubbell JA. Photopolymerized hyaluronic acid-based hydrogels and interpenetrating networks. *Biomaterials*. 2003;24(6):893-900.
29. Büttner M, Möller S, Keller M, Huster D, Schiller J, Schnabelrauch M, et al. Over-sulfated chondroitin sulfate derivatives induce osteogenic differentiation of hMSC independent of BMP-2 and TGF- β 1 signalling. *J Cell Physiol*. 2013;228(2):330-340.